Danicamtiv reduces myosin's working stroke but enhances contraction by activating the thin filament

Brent Scott[1], Lina Greenberg[1], Caterina Squarci[2], Kenneth S. Campbell[2], and Michael J. Greenberg[1,*]

[1]Department of Biochemistry and Molecular Biophysics, Washington University School of Medicine, St. Louis, MO, 63110, USA
[2] Division of Cardiovascular Medicine, University of Kentucky, Lexington, KY, 40506, USA

[*]Corresponding author:

Michael J. Greenberg
Department of Biochemistry and Molecular Biophysics
Washington University School of Medicine
660 S. Euclid Ave., Campus Box 8231
St. Louis, MO 63110
Phone: (314) 362-8670
Email: greenberg@wustl.edu

Keywords: single molecule, contractility, cardiac myosin

Running title: Danicamtiv's molecular effects

ABSTRACT

Heart failure is a leading cause of death worldwide, and even with current treatments, the 5-year transplant-free survival rate is only ~50-70%. As such, there is a need to develop new treatments for patients that improve survival and quality of life. Recently, there have been efforts to develop small molecules for heart failure that directly target components of the sarcomere, including cardiac myosin. One such molecule, danicamtiv, recently entered phase II clinical trials; however, its mechanism of action and direct effects on myosin's mechanics and kinetics are not well understood. Using optical trapping techniques, stopped flow transient kinetics, and *in vitro* reconstitution assays, we found that danicamtiv reduces the size of cardiac myosin's working stroke, and in contrast to studies in muscle fibers, we found that it does not affect actomyosin detachment kinetics at the level of individual crossbridges. We demonstrate that danicamtiv accelerates actomyosin association kinetics, leading to increased recruitment of myosin crossbridges and subsequent thin filament activation at physiologically-relevant calcium concentrations. Finally, we computationally model how the observed changes in mechanics and kinetics at the level of single crossbridges contribute to increased cardiac contraction and improved diastolic function compared to the related myotrope, omecamtiv mecarbil. Taken together, our results have important implications for the design of new sarcomeric-targeting compounds for heart failure.

44 **SIGNIFICANCE STATEMENT**

45 Heart failure is a leading cause of death worldwide, and there is a need to develop new
46 treatments that improve outcomes for patients. Recently, the myosin-binding small molecule
47 danicamtiv entered clinical trials for heart failure; however, its mechanism at the level of
48 single myosin crossbridges is not well understood. We determined the molecular
49 mechanism of danicamtiv and showed how drug-induced molecular changes can
50 mechanistically increase heart contraction. Moreover, we demonstrate fundamental
51 differences between danicamtiv and the related myosin-binding small molecule omecamtiv
52 mecarbil that explain the improved diastolic function seen with danicamtiv. Our results have
53 important implications for the design of new therapeutics for heart failure.

54 **INTRODUCTION**

55 Heart failure, a leading cause of mortality and morbidity in the world, is characterized
56 by the inability of the heart to generate sufficient power to perfuse the body at normal filling
57 pressures. Heart failure with reduced ejection fraction (HFrEF) is characterized by reduced
58 contractility during systole, and it accounts for ~50% of heart failure cases (1). Current
59 treatments for HFrEF (e.g., beta blockers and ACE inhibitors) target adverse remodeling of
60 the heart, which occurs secondary to reduced contractile function. While targeting adverse
61 remodeling has significantly improved outcomes for patients with HFrEF, the 5-year
62 transplant-free survival rates are still only ~50-70% (2). Thus, there is an outstanding need
63 to develop new therapeutics that improve mortality and quality of life for patients with HFrEF.

64 There has been a long-standing interest in developing heart failure treatments that
65 reverse the reduced contractile function seen in patients with HFrEF, but this approach has
66 been met with several challenges. Inotropes, such as milronone, increase heart contractility
67 by modulating calcium flux; however, elevated calcium leads to increased mortality (3), and
68 as such, inotropes are typically only used with patients in end-stage heart failure (1).
69 Recently, there have been several efforts to develop small molecules that directly target the
70 sarcomeric machinery to increase cardiac contraction without affecting calcium handling (4-
71 9). The first of these drugs was omecamtiv mecarbil (OM) (4), which was discovered in a
72 high-throughput screen for small molecules that increase cardiac myosin's ATPase activity.
73 OM made it to phase III clinical trials (10); however, the FDA declined to approve OM due to
74 its limited effect size and negative effects on relaxation.

75 Recently, a new myosin-binding compound was reported, danicamtiv, and this small
76 molecule is currently in phase II clinical trials for HFrEF (11). Currently, there is limited
77 information about the mechanism of danicamtiv, and the direct molecular effects of
78 danicamtiv on the kinetics and mechanics of individual myosin crossbridges is poorly
79 understood. In a study comparing OM and danicamtiv, it was reported that danicamtiv has

a smaller impact on relaxation compared to OM (9); however, the molecular mechanism underlying this difference is not known. Moreover, elegant experiments in muscle fibers and myofibrils have shown clear structural and functional effects of danicamtiv at the cellular and sub-cellular levels (12-14). X-ray diffraction of danicamtiv treated muscle fibers revealed an increase in filament lattice spacing and a re-positioning of myosin heads closer towards the thin filament (14). Moreover, danicamtiv was shown to slow the rate of tension development in porcine myofibrils (14), slow tension redevelopment in human myocardial bundles (13), slow the rate of myofibril relaxation (14), and slow the rate of myosin-driven motility *in vitro* (14). Based on these observations, it was suggested that danicamtiv likely slows the rate of ADP release from actomyosin, the transition that limits actomyosin dissociation in cycling muscle; however, the direct effects of danicamtiv at the level of single crossbridges has not been examined.

Here, we use a combination of stopped flow transient kinetics, single molecule optical trapping, computational modeling, and in vitro reconstitution assays to directly measure how danicamtiv affects the mechanics and kinetics of individual myosin crossbridges. Our results provide new insights into the mechanism of danicamtiv and help to explain its differences with OM.

100 **RESULTS**

101 We set out to measure the effects of danicamtiv on the mechanics and kinetics of
102 individual cardiac myosin crossbridges. We used porcine cardiac actin, which is identical to
103 the human isoform, and porcine ventricular cardiac myosin which has biophysical properties
104 that are indistinguishable from human cardiac myosin (15-17). Danicamtiv was dissolved in
105 DMSO (10 mM) and diluted in KMg25 Buffer to a final concentration of 10 μM for all
106 experiments. The final experiment buffers contained 0.1% DMSO. First, we examined the
107 effects of danicamtiv on myosin's steady-state ATPase activity. Similar to previous reports
108 using isolated myofibrils (11), we found that danicamtiv increases myosin's maximal steady-
109 state ATPase rate at saturating actin by ~1.2-fold (P = 0.028) and increases the effective K_m
110 (P = 0.01) (**Fig. 1A, Table 1**). Next, we used an *in vitro* motility assay in which fluorescently
111 labeled actin is translocated over a bed of myosin in the presence of ATP (18) and we
112 measured the speed of myosin-based movement. Consistent with previous reports, we
113 observed that danicamtiv reduces the motile speed by ~55% (**Fig. 1B**) (P = $4x10^{-6}$). Taken
114 together, danicamtiv accelerates the overall rate of myosin crossbridge cycling kinetics while
115 reducing the speed at which it moves actin.

116

117 **Danicamtiv does not affect key biochemical transitions that govern actomyosin**
118 **detachment (ADP release or ATP-induced dissociation)**

119 Our data demonstrate that danicamtiv increases overall cycling kinetics while
120 simultaneously reducing the speed of myosin motility, suggesting that danicamtiv affects the
121 coupling between the mechanics and kinetics of myosin crossbridges. In the motility assay,
122 the speed of actin filament translocation is proportional to the displacement generated by a
123 single myosin (i.e., the size of the myosin working stroke) divided by the amount of time that
124 myosin remains attached to the actin filament (19):

125 $$\text{speed} \propto \text{displacement} / \text{attachment time} \qquad \text{Eq. 1}$$

126 Thus, the ~50% reduction in motile speed suggests that either the displacement generated
127 by the myosin is reduced by half or the attachment time of a crossbridge gets twice as long.
128 Therefore, we set out to directly test these two possibilities.

129 To test whether danicamtiv affects the time that crossbridges remain bound to actin,
130 we measured the rates of key biochemical transitions. The amount of time that actin and
131 myosin remain attached is set by the time required for ADP release and subsequent ATP-
132 induced actomyosin dissociation (20). Since the rate of a transition is inversely proportional
133 to the average time for the transition to occur, we can equivalently state that the rate of
134 crossbridge dissociation is set by the rates of ADP release from myosin and ATP-induced
135 dissociation of actomyosin (**Fig. 1C**). Therefore, we measured the rates of these transitions
136 using stopped flow transient kinetics.

137 First, we measured the rate of ATP-induced actomyosin dissociation using pyrene-
138 labeled actin as a fluorescent reporter of actomyosin binding (21), where myosin detachment
139 from pyrene-labeled actin causes an increase in pyrene fluorescence. We rapidly mixed
140 pyrene-labeled actomyosin with a range of ATP concentrations and measured the change
141 in fluorescence. As previously described, fluorescence transients were well fitted by the
142 sum of two exponential functions, where the observed rate of the fast phase can be used to
143 report the rate of ATP-induced actomyosin dissociation (21). The relationship between the
144 observed rate of the fast phase and the concentration of ATP was fitted with a hyperbolic
145 function to obtain the maximal rate of ATP-induced dissociation at saturating ATP
146 concentrations, k_{+2}', and the concentration of ATP necessary to reach half-maximal
147 saturation, $1/K_1$' (**Fig. 2A**). We found that danicamtiv does not affect the maximal rate of
148 ATP-induced dissociation (P = 0.99), the concentration of ATP necessary to reach half-
149 maximal saturation (P = 0.64), or the second-order rate of ATP induced dissociation (4.0 ±
150 0.7 vs 4.4 ± 1.1 $\mu M^{-1}s^{-1}$, for 0 and 10 μM danicamtiv, P = 0.64) (**Table 1**). Thus, changes in

151 ATP-induced actomyosin dissociation cannot explain the reduced motility seen with
152 danicamtiv.

153 Next, we measured the rate of ADP release from actomyosin by preparing a mixture
154 of ADP-saturated myosin and pyrene-labeled actin, and rapidly mixing this with saturating
155 amounts of ATP, leading to an increase in fluorescence (21). The fluorescence transients
156 were fitted with single exponential functions to obtain the rate of ADP release from
157 actomyosin (**Fig. 2B**). We found that the rates of ADP release with and without 10 μM
158 danicamtiv were not statistically different (WT: 73 ± 3 s^{-1}, Danicamtiv: 73 ± 3 s^{-1}, P = 0.96).
159 This rate of ADP release is consistent with previous measurements using porcine β-cardiac
160 myosin (16, 22) and recombinant human cardiac myosin (23). Moreover, at physiologically
161 relevant saturating ATP concentrations, the rate of ADP release is slower than the rate of
162 ATP-induced actomyosin dissociation both in the presence and absence of danicamtiv. As
163 such, the rate of ADP release limits actomyosin dissociation at saturating ATP
164 concentrations, such as those in the motility assay and in cardiomyocytes. Taken together,
165 the observed reduction in motile speed cannot be explained by changes in the rate of ADP
166 release from actomyosin.

167 It has also been proposed that danicamtiv might affect the rate of ADP binding to
168 actomyosin (14). To test this, we determined the ADP binding affinity to actomyosin by
169 measuring the rate of pyrene-actomyosin dissociation in the presence of competing mixtures
170 of ATP and ADP (21). We found that the ADP affinity was not statistically different with or
171 without danicamtiv (**Fig. 2C**; P = 0.87). Moreover, we can use this affinity and the measured
172 ADP release rate to calculate the rate of ADP binding (k_{-5}' see Methods for details), and we
173 found that there is no statistical difference in the rate of ADP rebinding with danicamtiv (P =
174 0.4). Taken together, we did not observe changes in the rates of key steps of actomyosin
175 dissociation that could explain the reduction in motile speed.

176 Finally, we measured the rate of ATP hydrolysis by myosin across a range of ATP
177 concentrations using the intrinsic tryptophan fluorescence of the myosin which increases
178 with hydrolysis (**Fig. 2D**) (21). We found that the observed fluorescence transients are well
179 fitted by a single exponential function. When plotting the observed rates against their
180 respective ATP concentrations, the data is well described by a hyperbolic function where the
181 plateau represents the sum of the forwards and backwards rates of ATP hydrolysis. Our
182 measured rate of ATP hydrolysis by porcine cardiac myosin (79.8 ± 3.0 s^{-1}) is consistent with
183 previous reports (23). While there was a slight decrease in the observed hydrolysis rate with
184 danicamtiv (79.8 ± 3.0 vs. 72.6 ± 2.5 s^{-1}, for DMSO control and danicamtiv, respectively; P
185 = 0.03), this small decrease is not biologically meaningful, and it cannot not explain the
186 differences see with the ATPase rate or motility.
187
188 **Danicamtiv reduces the displacement of myosin's working stroke without altering**
189 **detachment kinetics**
190 Given that we did not observe a change in biochemical kinetics that could explain the
191 ~50% reduction in motile speed with danicamtiv (**Fig. 1B**), we used single molecule optical
192 trapping techniques to measure the mechanics of the cardiac myosin working stroke in the
193 presence and absence of danicamtiv (16, 24). We used the three-bead assay in which an
194 actin filament is suspended between two optically-trapped beads and lowered onto a
195 surface-bound pedestal that is sparsely coated with myosin (25) (**Fig. 3A**). We were able
196 to clearly resolve single molecule interactions between actin and myosin (**Fig. 3B**), enabling
197 us to probe the mechanics and kinetics of the myosin working stroke.
198 First, we measured single molecule interactions between actin and myosin at low,
199 non-physiological ATP concentrations (10 μM ATP) to facilitate the observation of substeps
200 of the myosin working stroke. The size of the working stroke can be measured by fitting
201 single exponential functions to the time forward ensemble averages (**Fig. 3C**) or by

202 calculating the relative position change that occurs with each actomyosin interaction (**Fig.**
203 **3D**). Both analyses provide similar results (**Table 2**). We found that in the absence of
204 danicamtiv, cardiac myosin has a working stroke size of 5.0 nm, consistent with previous
205 measurements of human and porcine cardiac myosins (15-17, 26). We found that in the
206 presence of danicamtiv, the total size of myosin's working stroke was reduced to 2.5 nm (P
207 < 0.01; **Fig. 3C**). This ~50% reduction in the working stroke displacement is consistent with
208 the 55% decrease in speed we observed in motility (**Fig. 1B**).

209 Optical trapping also enables the direct measurement of the actomyosin attachment
210 duration. Cumulative distributions of attachment durations were generated and fitted with a
211 single exponential function to obtain the rate of actomyosin detachment (**Fig. 3E**). We found
212 that the detachment rate in the absence of danicamtiv at 10 μM ATP was 23 (-2.5/+2.5) s^{-1},
213 consistent with the expected rate of detachment based on the stopped flow measurements
214 (**Fig. 2**). Moreover, we found that there was no statistically significant difference in the
215 actomyosin detachment rate in the presence of danicamtiv at 10 μM ATP compared to the
216 DMSO control (24 (-0.8/+0.9) s^{-1}, $P = 0.39$, **Fig. 3E**), consistent with our stopped flow
217 measurements which suggested that danicamtiv does not change actomyosin detachment
218 kinetics. This result contrasts with OM. Consistent with previous studies, we show that OM
219 further reduces the size of the working stroke compared to danicamtiv and significantly slows
220 the rate of actomyosin dissociation in the optical trap (**Supp. Fig. 1**) (15). Taken together,
221 our results suggest that unlike OM, danicamtiv does not affect the kinetics of actomyosin
222 detachment at the single molecule level at low ATP.

223 To ensure that our observations in the optical trap at 10 μM ATP were not a result of
224 working at low ATP concentrations, we also collected an additional optical trapping dataset
225 at a physiologically-relevant saturating ATP concentration (1 mM) (**Supp. Fig. 2**). At 1 mM
226 ATP we observed that myosin's displacement is reduced ~50% with danicamtiv ($P < 0.01$).
227 Moreover, we do not observe a difference in the actomyosin detachment rate with danicamtiv

228 (P = 0.15, **Table 2**), consistent with our observations at low ATP and the stopped flow
229 measurements.

230 Next, we tested whether danicamtiv affects myosin's load-dependent detachment
231 kinetics at the level of single molecules at 1 mM ATP (**Fig. 4A**). To do this, we used a
232 feedback loop to exert force on the myosin during its working stroke, and we measured the
233 actomyosin attachment duration under load (16). The relationship between force and
234 attachment duration can be fit to extract the rate of the primary force-sensitive transition in
235 the absence of force, k_0, and the distance to the transition state (a measure of force
236 sensitivity) (**Fig. 4B**) (27). We found that at saturating ATP concentrations, the rate of the
237 primary force sensitive transition in the absence of danicamtiv was 61 (-21/+40) s^{-1},
238 consistent with the rate of ADP release measured in the stopped flow (**Fig. 2B**) and previous
239 measurements (16, 26), and this rate was not statistically different in the presence of
240 danicamtiv (89 (-18/+24) s^{-1}, P = 0.12). Moreover, the distance to the transition state was
241 not statistically different in the absence or presence of danicamtiv (d = 1.4 (-0.37/+0.46) nm
242 vs 1.25 (0-.16/+0.17) nm, respectively, P = 0.35). Thus, danicamtiv does not change the
243 load-dependent kinetics of cardiac myosin at physiologically-relevant ATP concentrations,
244 and the observed reduction in motile speed (**Fig. 1B**) can be explained by a reduction in the
245 size of the myosin working stroke (**Fig. 3C**).

246

247 **Danicamtiv increases the kinetics of actomyosin attachment**

248 Our results clearly demonstrate that at the level of single crossbridges, danicamtiv
249 does not affect actomyosin detachment kinetics. Therefore, we investigated whether
250 danicamtiv affects actomyosin attachment kinetics. Our steady-state ATPase
251 measurements (**Fig. 1A**) demonstrate that danicamtiv increases the overall steady-state
252 ATPase rate, indicative of the fact that danicamtiv increases the rate of the slowest step of
253 the ATPase cycle. For β-cardiac myosin cycling in the presence of actin, the overall cycle

254 rate is limited by attachment kinetics (23). Since danicamtiv increases the steady state
255 ATPase without altering detachment kinetics, we posited the increase in ATPase could be a
256 result of danicamtiv accelerating attachment kinetics.

257 To test whether danicamtiv affects attachment kinetics, we used stopped flow
258 techniques to measure the rates of actomyosin attachment and detachment under single
259 turnover conditions (28) (**Fig. 5A,** see Supplemental Materials for additional details). Myosin
260 was preincubated with an excess of pyrene-labeled actin to form a rigor complex that
261 quenches pyrene's fluorescence. The actomyosin was then rapidly mixed with a sub-
262 saturating concentration of ATP, causing an increase in fluorescence that reports the
263 actomyosin detachment rate at this ATP concentration, k_{det}. A low concentration of ATP is
264 used to ensure that this process only occurs once (i.e., a single turnover). Once off actin,
265 myosin hydrolyzes ATP and then re-attaches to actin, quenching the pyrene fluorescence
266 and reporting the rate of myosin attachment at this actin concentration, k_{att}.

267 The single turnover fluorescence transients consisted of two phases, where the rate
268 of detachment was faster than the rate of attachment, consistent with the notion that the rate
269 of attachment limits the overall ATPase cycle time (**Fig. 5B, Supp. Figs. 3 and 4**). We saw
270 that there was no statistically significant difference in the rate of detachment in DMSO or
271 danicamtiv. (3.8 ± 0.9 vs 4.2 ± 0.8 s^{-1}, respectively, P = 0.23, **Fig. 5C**). This measured
272 detachment rate is in agreement with the second-order rate of ATP-induced dissociation at
273 0.75 μM ATP measured in the stopped flow (**Table 1**). We also saw that the observed
274 attachment rate was significantly faster with 10 μM compared to DMSO controls (0.0040 ±
275 0.0002 vs 0.0063 ± 0.0006 $\mu M^{-1} \cdot s^{-1}$, respectively, P < 0.001, **Fig. 5D**). Taken together, our
276 data demonstrate that danicamtiv increases attachment kinetics without affecting
277 detachment kinetics.

278

279 **Danicamtiv-induced increase in the myosin attachment rate causes increased thin**
280 **filament activation**

281 Given that danicamtiv increases the attachment rate of myosin to actin, we
282 hypothesized that this would lead to an increase in the fraction of myosin heads bound to
283 actin (i.e., the duty ratio). To test this hypothesis, we used a well-established variation of the
284 *in vitro* motility assay where the speed of actin filament movement was measured as a
285 function of surface myosin (29, 30). Actin filaments move at their maximal speed if there is
286 a sufficient concentration of myosin on the surface to ensure that at least one myosin head
287 is attached to the filament at any given time. We observed that despite moving slower,
288 danicamtiv-treated myosin required less myosin to reach saturation, consistent with an
289 increased duty ratio with drug (**Figs. 6A and B**).

290 Given the increase in the rate of myosin binding to actin with danicamtiv, we
291 hypothesized that danicamtiv would increase myosin-induced thin filament activation, since
292 thin filament activation depends on myosin binding (31). To test this, we reconstituted thin-
293 filaments in the *in vitro* motility assay, and we measured the speed of myosin-based
294 translocation over a range of calcium concentrations. We saw that danicamtiv increased thin
295 filament motility at submaximal calcium levels where the motility speed is limited by the rate
296 of myosin attachment (e.g. at pCa 7, 16 ± 28 vs. 51 ± 31 nm/s, $P < 0.001$) (**Fig. 6C**). These
297 low calcium levels are within the physiological range of calcium concentrations seen in
298 muscle (32). Taken together, our data suggest that danicamtiv-induced increases in
299 attachment kinetics lead to increased thin filament activation at submaximal calcium
300 concentrations.

301

302 **Computational modeling connects molecular effects and muscle function**

303 To better understand how changes at the molecular scale with danicamtiv would
304 translate into altered muscle contraction, we used computational modeling. We used a

305 spatially explicit model of muscle contraction, FiberSim (33). This model has previously
306 been used to successfully model several physiologically important parameters, including the
307 force-calcium relationship and the force generated in response to a calcium transient.

308 We used FiberSim to model the effects of danicamtiv on key muscle parameters
309 based on our molecular measurements. Our results show that danicamtiv reduces the size
310 of the working stroke while increasing the rate of crossbridge attachment. Moreover,
311 previous X-ray diffraction studies have shown that danicamtiv causes myosin to transition
312 from an autoinhibited interacting heads motif to an activated disordered relaxed state (14).
313 We adjusted the model input parameters to match these changes, and we simulated the
314 effects of each of these changes in isolation (**Supp. Fig. 5**) and all together (**Figs. 6E and**
315 **F**). We simulated both the force-calcium relationship and the force generated in response to
316 a calcium transient. When looking at the composite effects of all three changes, we see that
317 this causes a shift in the force calcium relationship towards submaximal calcium activation
318 (**Fig. 6E**) that agrees well with our experimental measurements (**Fig. 6D**). Moreover, the
319 modeling shows that danicamtiv is expected to increase both the magnitude of the force
320 generated in response to a calcium transient with slight slowing of both the rates of force
321 development and relaxation (**Fig. 6F**). Finally, the modeling predicts that danicamtiv will
322 increase the force-time integral (**Fig. 6G**). Taken together, our modeling provides insights
323 into how danicamtiv affects the kinetics and mechanics of myosin, leading to increased
324 muscle function.

DISCUSSION

At the level of single crossbridges, danicamtiv's biophysical mechanism is more complicated than a "myosin activator"

Our observation of ~50% reduced motility with danicamtiv (**Fig. 1B**) is consistent with the excellent study by Kooiker et al. (14). Previously, it was suggested that this reduced speed could be due to danicamtiv's effects on ADP binding and release, since the rate of ADP release limits the shortening speed of muscle (34). We directly measured the rate of ADP binding, rate of ADP release, and the equilibrium constant for ADP binding, and we do not see changes in any of these parameters (**Figs. 2B and C**). Moreover, we directly measured the rate of actomyosin dissociation in the optical trap at both high and low ATP concentrations, and we did not observe any changes in the detachment rate (**Fig. 3E**). We also measured the load-dependent detachment kinetics in the optical trap, and we did not observe any changes with danicamtiv treatment (**Fig. 4**). Finally, we used a single turnover stopped flow assay, and we do not see any difference in the detachment kinetics (**Fig. 5C)** Taken together, our results demonstrate that danicamtiv does not have effects on the rate of ADP release or actomyosin detachment at the level of single crossbridges.

The speed in the motility assay is proportional to the step size of the myosin divided by the amount of time that the crossbridge remains attached (19). While we did not observe any changes in attachment time in the optical trap, we did observe a ~50% decrease in the size of the myosin working stroke (**Fig. 3E**). As such, the ~50% decrease in motility speed can be explained by a ~50% reduction in the size of the working stroke. Taken together, at the level of individual crossbridges, the reduced speed in motility seen with danicamtiv cannot be explained by changes in detachment kinetics, rather, it is due to a decrease in the size of the myosin working stroke.

350 Danicamtiv was initially discovered in a high-throughput screen for molecules that
351 activate the steady-state ATPase activity of myosin, and as such, it was initially classified as
352 a myosin activator (11); however, as we show here, it has a more complex biophysical
353 mechanism at the level of single crossbridges. The ATPase assay uses a minimal number
354 of components (i.e., myosin, actin, and ATP) to measure the steady-state rate of ATP
355 turnover. While this assay is useful for drug screening due to its well-characterized and
356 easily measured outputs, it also has important limitations due to its simplified nature. This
357 assay considers only the effects of drugs on kinetics, and it does not consider effects on
358 mechanics or incorporate higher-order structures that are important for muscle function
359 (e.g., sarcomere lattice, myosin autoinhibition in the thick filament, calcium-based
360 regulation). This limitation becomes clear in the case of danicamtiv, where mechanics and
361 kinetics are uncoupled. We show that danicamtiv is an activator of myosin's steady-state
362 ATPase rate (**Fig. 1A**), but an inhibitor of myosin mechanics (**Fig. 3C**). This demonstrates
363 that danicamtiv partially uncouples myosin mechanics and kinetics, and its biophysical
364 mechanism is more complicated than a simple myosin activator. We propose that
365 danicamtiv should be classified as a myosin-binding sarcomeric activator.
366

367 **Danicamtiv's activating properties emerge in higher-order structures**

368 Since danicamtiv has both inhibitory and activating effects at the level of individual
369 crossbridges, we further investigated its effects in higher-order structures. Increased
370 cardiac contractility has been observed in muscle fibers, small animal models, and humans
371 (9, 11-14, 35). One difference between actomyosin in isolation and in muscle is the
372 presence of the thin filament regulatory proteins, tropomyosin and troponin. In the absence
373 of calcium, tropomyosin blocks the myosin strong binding sites on actin, preventing myosin
374 attachment and subsequent force generation (36). During systole, calcium binds to troponin,
375 leading to movement of tropomyosin followed by attachment of myosin crossbridges. Thus,

376 the process of thin filament activation depends both on both calcium and myosin binding to
377 the thin filament.

378 Here, we observed that danicamtiv increases the rate of myosin attachment to actin
379 (**Figs. 1A and 5D**). As such, we hypothesized that increased attachment would lead to
380 increased binding to the thin filament, causing activation of the thin filament at submaximal
381 calcium levels. In fact, this is what we observe in the *in vitro* motility assay using regulated
382 thin filaments, and similar shifts were seen in muscle fiber experiments (12-14). To test
383 whether this increased myosin attachment could contribute to the observed changes in
384 muscle fiber force, we performed computational modeling of the sarcomere using FiberSim
385 (**Fig. 6E**). We found that changing myosin's rate of attachment to the thin filament alone is
386 sufficient to recapitulate the shift towards submaximal calcium activation that we observed
387 in the *in vitro* motility assay (**Supp. Fig. 5**). Taken together, we propose that danicamtiv
388 increases muscle contraction, in part, through activation of the thin filament.

389 As mentioned above, simplified systems cannot capture all aspects of cardiac
390 contraction, and previous studies in muscle fibers have demonstrated several effects that
391 we cannot observe at the level of individual crossbridges (12-14). To gain some insights
392 into how changes at the level of individual crossbridges translates into muscle function, we
393 used a spatially explicit model of muscle contraction to simulate key physiological
394 parameters (**Figs. 6E and F** and **Supp. Fig. 5**). We simulated the individual and composite
395 effects of (1) increased crossbridge attachment based on **Figs. 1A** and **5D**, (2) decreased
396 working stroke size based on **Figs. 1B** and **3C**, and (3) an increase in the number of myosin
397 crossbridges available to interact with the thin filament based on X-ray diffraction studies of
398 muscle fibers (14). Our results clearly demonstrate that these danicamtiv-induced changes
399 at the level of single crossbridges are sufficient to reproduce the shift towards submaximal
400 calcium activation, increased peak force production in response to a calcium transient, and
401 an increase in the force-time integral. Moreover, we observe slightly slowed rates of force

402 development and relaxation with danicamtiv that emerge without changes in the rate of
403 crossbridge detachment. Taken together, our results demonstrate the importance of
404 multiscale studies for understanding the mechanisms of small molecules targeting myosin.
405

406 **Comparison with omecamtiv mecarbil**

407 The first compound targeting cardiac myosin for the treatment of systolic heart failure
408 was omecamtiv mecarbil (OM) (5, 6). Like danicamtiv, OM was also identified in a screen
409 for small molecules that increase myosin's steady-state ATPase activity. OM made it to
410 stage III clinical trials, but ultimately the FDA declined to approve OM due to its limited effect
411 size and its impact on cardiac relaxation (10). In particular, patients treated with OM showed
412 prolonged systole and impaired relaxation, which lead to an increase in serum troponin,
413 indicative of cardiac damage.

414 There are some similarities between OM and danicamtiv seen at the molecular scale.
415 Both danicamtiv and omecamtiv increase myosin's ATPase activity and slow the rate of
416 motility (5, 37). Both danicamtiv and OM decrease the size of the myosin working stroke
417 (15); however, the reduction in the size of the working stroke with danicamtiv was not as
418 severe as the reduction caused by OM (**Supp. Fig. 1C**). The decrease in size of the working
419 stroke can be seen for both OM and danicamtiv; however, this effect is more pronounced
420 for OM which almost completely eliminates the working stroke.

421 The key difference between OM and danicamtiv is that omecamtiv significantly
422 increases the amount of time that actin and myosin remain attached while danicamtiv does
423 not. This can be seen in **Supp. Fig 1D**. This subtle difference has important implications for
424 the mechanism of action. OM increases the attachment duration, leading to slowed
425 detachment of myosins, prolonging systole. This effect would not be expected for
426 danicamtiv, suggesting that it might have better effects on relaxation and diastolic function.
427 Consistent with this notion, experiments using engineered heart tissues and muscle fibers

428 showed that danicamtiv has a lower impact on relaxation than OM (9, 13). It is worth noting
429 however, that while the effects of danicamtiv on diastolic function are smaller that OM, they
430 still exist (9, 35), and we can observe evidence of slowed relaxation in our computational
431 modeling. It remains a challenge to the field to develop small molecules that can uncouple
432 myosin's effects on systole and diastole.
433

434 **Conclusions**

435 Here, we demonstrate the effects of danicamtiv on single crossbridges and highlight
436 how properties at the single molecule level translate into effects seen in muscle fibers.
437 Importantly, our results demonstrate that danicamtiv is a myosin binding sarcomeric
438 activator that exerts its effects in part through thin filament activation.

Acknowledgements:

The authors acknowledge financial support provided by the National Institutes of Health (R01 HL141086 to M.J.G., R01 HL148785 to K.S.C., T32 HL125241 to B.S.), the Children's Discovery Institute of Washington University and St. Louis Children's Hospital (PM-LI-2019-829 M.J.G.), and the American Heart Association (TPA 970198 to M.J.G).

Conflict of interest statement:

All experiments were conducted in the absence of any commercial or financial relationships that could be construed as potential conflicts of interest. M.J.G. discloses research funding from Edgewise Therapeutics on an unrelated project.

Author contributions:

Conception and oversight by M.J.G.. ATPase experiments were conducted by L.G.. Computational modeling was conducted by C.S., K.S.C., and B.S.. All single molecule and transient kinetic experiments were conducted by B.S.. All authors contributed to the analysis of the data. The first draft was written by M.J.G.. All authors contributed to the writing and/or editing of the manuscript.

456 **MATERIALS AND METHODS**

457

458 Full experimental procedures can be found in the Supplemental Materials.

459

460 **Biochemical Kinetic Measurements**

461 Porcine ventricular actin and myosin were purified from tissue, and human troponin and
462 tropomyosin were recombinantly expressed in *E. coli* (22). Actin was labeled with pyrene
463 as previously described (22). Danicamtiv was purchased from Selleckchem (99.1% purity,
464 S9948). ATPase measurements as a function of actin concentration were conducted using
465 the NADH enzyme coupled assay (21, 38). Stopped flow measurements were conducted
466 in an SX-20 instrument (Applied Photophysics). Using these techniques, we measured the
467 rates of ATP induced actomyosin dissociation, ADP release, ADP hydrolysis, ADP binding
468 affinity, and single turnover kinetics (21).

469

470 ***In Vitro* Motility and Optical Trapping Experiments**

471 *In vitro* motility assays were conducted as previously described, where actin filaments
472 translocate over a bed of myosin in the presence of ATP (39, 40). Thin filament regulation
473 was reconstituted by adding calcium and the regulatory proteins troponin and tropomyosin.
474 Optical trapping was done using the three-bead assay in which an actin filament is stretched
475 between two optically trapped beads and lowered on to a pedestal bead that is sparsely
476 coated with myosin (16, 24, 27). Data were analyzed using the SPASM software (24).

477

478 **Computational modeling**

479 Computational modeling was done using FiberSim, a spatially explicit model of muscle
480 contraction (33). Model input parameters were modified to match experimental

measurements. The force-calcium relationship and the time-dependent response to a calcium transient were simulated.

Data Availability and Reproducibility

All data is included in the project repository hosted on Zenodo (10.5281/zenodo.12636349). All analysis was performed in R version 4.4.0 (R Core Team) unless otherwise noted. The code has been made available to reproduce verbatim all figures and related analyses in the project repository.

489 **Figure Legends**

490

491 **Figure 1. Steady state properties of β-cardiac myosin treated with danicamtiv. A)** The
492 steady-state myosin ATPase rate was measured using the NADH coupled assay. The
493 steady state myosin ATPase rate is plotted verses a function of actin concentration. Data
494 were fitted by a hyperbolic function to calculate the maximal cycling rate (V_{max}) and actin
495 affinity (K_m) with the Michaelis Menten equation. Treatment with 10 μM danicamtiv increased
496 the maximal rate by ~1.2 fold from 5.9 to 7.0 s^{-1} (P = 0.028) and decreased the K_m from 14.0
497 to 8.1 μM (P = 0.01). Each point represents the average rate from four independent trials
498 with error bars showing the standard deviation. Statistical testing done using a 2-tailed T-
499 test. Black = DMSO control. Pink = 10 μM danicamtiv. **B)** Speed of actin translocation in the
500 unregulated in vitro motility assay. The addition of 10 μM danicamtiv decreased motility
501 speed ~55% (P = $4x10^{-6}$). Thick horizontal lines show the average speed with standard
502 deviation shown by the thin horizontal lines. Points represent the average speed of all
503 filaments in a field of view for a single technical replicate measured across N = 3
504 independent experiments. Statistical testing done using a 2-tailed T-test. **C)** Scheme of
505 myosin's mechanochemical cross-bridge cycle. Myosin's rate limiting step is actin
506 attachment, so the predominant population of motors reside in the pre-working stroke
507 M.ADP.Pi state during steady state cycling. The steady-state ATPase is thus limited by actin
508 attachment (k_{att}) which is rapidly followed by the mechanical working stroke and phosphate
509 release. *In vitro* motility speed is limited by the ADP release rate (k_{+5}').

510

511 **Figure 2. Stopped-flow kinetics measured with and without 10 μM danicamtiv.** Black
512 = DMSO control. Pink = 10 μM danicamtiv. **A)** The rates of ATP-induced actomyosin
513 dissociation were measured in the stopped flow. Transients were well fitted by the sum of
514 two exponential functions, where the observed rate of the fast phase (k_{fast}) is plotted as a

515 function of ATP concentration. Data were fitted with a hyperbolic function to obtain K_1' and
516 k_{+2}'. There are no differences in either K_1' or k_{+2}' with or without danicamtiv (P = 0.64 and P
517 = 0.99, respectively). Each point represents an independent measurement over 3
518 experimental days. **B)** The rate of ADP release from actomyosin was measured using
519 stopped flow techniques, and the fluorescence transients were fitted with single exponential
520 functions. Note, both 0 and 10 μM danicamtiv are plotted and overlay. There is no statistically
521 significant difference in the rate of ADP release the absence or presence of danicamtiv (P =
522 0.96). **C)** The overall ADP binding affinity to actomyosin was measured by mixing an
523 actomyosin solution containing increasing concentrations of ADP with 50 μM ATP
524 (concentrations after mixing) measured using a competition experiment. The observed rate
525 as a function of ADP concentration was fitted with a hyperbolic function to determine the
526 ADP affinity (see methods). Each point shows the average of 3 separate trials and error bars
527 show the standard deviations. There is no difference in the ADP binding affinity (k_{-5}'; P =
528 0.40). **D)** The rate of ATP hydrolysis by myosin was measured using stopped flow
529 techniques. The rate of hydrolysis is reported by the change in tryptophan fluorescence at
530 saturating ATP concentrations. Fluorescence transients are well fitted with single
531 exponential functions. The observed rates of ATP hydrolysis were plotted against their
532 respective ATP concentration and fitted with a hyperbolic function. The plateau represents
533 the sum of the forwards and backwards rate of ATP hydrolysis (k_3 *(obs)*). While there was a
534 slight decrease in the observed hydrolysis rate with danicamtiv (P = 0.03), this slight
535 decrease is not biologically meaningful. For all stopped-flow values, see **Table 1**.
536
537 **Figure 3. Single molecule optical trapping reveals that danicamtiv reduces the size of**
538 **myosin's working stroke without altering detachment kinetics.** Black = DMSO control.
539 Pink = 10 μM danicamtiv. **A)** Cartoon schematic of the optical trapping assay. An actin
540 filament is strung between two optically-trapped beads and lowered onto a pedestal bead

541 sparsely bound with myosin. **B)** Optical trapping data traces showing the stochastic binding
542 of myosin to actin. Binding interactions are shown in grey or pink and detached states are
543 shown in black. **C)** Time forward ensemble averages of myosin's working stroke reveal a
544 ~50% reduction in the size of myosin's total working stroke in the presence of danicamtiv.
545 **D)** The cumulative distribution of the total working stroke displacements at 10 μM ATP is well
546 fit by a single cumulative Gaussian function (dotted lines) with average values of 4.9 ± 9.7
547 nm versus 3.0 ± 9.0 nm for DMSO control and 10 μM danicamtiv, respectively ($P < 0.001$
548 using a two-tailed T-test). N = 2076 binding interactions for control and 4776 binding events
549 for 10 μM danicamtiv. **E)** The cumulative distributions of attachment durations at 10 μM ATP.
550 Single exponential functions were fit to the distributions using maximum likelihood
551 estimation. 95% confidence intervals were calculated using bootstrapping methods. There
552 is no statistical difference between control and 10 μM danicamtiv, 23 (-2.5/+2.5) s^{-1} vs. 24 (-
553 0.8/+0.9) s^{-1} ($P = 0.48$). For all trapping values, see **Table 2**.
554
555 **Figure 4. Danicamtiv does not alter myosin's load-dependent detachment kinetics at**
556 **1 mM ATP.** Black = DMSO control. Pink = 10 μM danicamtiv. **A)** An isometric force clamp
557 was used to maintain actin at an isometric position during myosin binding interactions. To
558 do this, the motor bead (M) was moved to hold the transducer bead (T) at an isometric
559 position. Data traces are shown. **B)** Plots of actomyosin attachment duration versus the
560 average resistive force applied during the binding event. Data are exponentially distributed
561 at each force. Each point represents an independent actomyosin binding interaction. The
562 data were fitted with the Bell equation using maximum likelihood estimation and 95%
563 confidence intervals were calculated for each parameter by bootstrapping. The detachment
564 rate in the absence of load, k_0, was not different between control and 10 μM danicamtiv, 61
565 (-21/+40) vs 89 (-18/+24) s^{-1} ($P = 0.17$). These values are consistent with our measurements
566 of the rates of ADP release from stopped-flow experiments. The distance to the transition

567 state, *d*, which measures the load-sensitivity of the detachment rate, was not different
568 between control and 10 μM danicamtiv, 1.40(-0.37/+0.46) vs 1.25 (-0.16/+0.17) nm (P =
569 0.43).
570
571 **Figure 5. Danicamtiv increases myosin's attachment rate in a single turnover stopped**
572 **flow assay.** Black = DMSO control. Pink = 10 μM danicamtiv. **A)** Schematic conceptually
573 describing the single turnover assay used to measure myosin's attachment and detachment
574 rates. In this assay, myosin and pyrene labeled actin are pre-incubated and then mixed with
575 a sub-saturating concentration of ATP. The pyrene fluorescence increases as myosins
576 detach from actin, and the increase in fluorescence reports the rate of detachment of myosin
577 from actin (k_{det}). Myosin then reattaches to actin, quenching the fluorescence and reporting
578 the attachment rate (k_{att}). **B)** Fluorescence transients from the single turnover assay. Data
579 were fitted as described in the Supplemental Methods. **C)** The average second-order rate
580 of detachment (k_{det}) was similar with and without 10 μM danicamtiv (3.8 ± 0.9 vs. 4.2 ± 0.8
581 s^{-1}; P = 0.23). **D)** The second-order rate of attachment (k_{att}) increased with the addition of 10
582 μM danicamtiv (0.0040 ± 0.0002 vs 0.0063 ± 0.0007 $\mu M^{-1} \cdot s^{-1}$; P = < 0.001). For **C** and **D**, the
583 thick lines show the average values, and the error bars show the standard deviation. The
584 individual points are the fitted second-order rates to individual transients collected across
585 three experimental replicates. Statistical testing was done using a two-tailed T-test after
586 passing a normality test.
587
588 **Figure 6. Danicamtiv increases motility speed in the presence of regulatory proteins**
589 **and these effects on muscle contraction can be recapitulated computationally.** Black
590 = DMSO control. Pink = 10 μM danicamtiv. **A and B)** Unregulated *in vitro* motility speed as
591 a function of the myosin concentration on the flowcell surface. The speed decreases if there
592 is not at least one active myosin head bound to actin at any given time. Thus, if the duty

593 ratio increases with drug, less myosin will be required to reach saturation. 10 μM danicamtiv
594 decreases motility speed at higher myosin concentrations but increases speed at low myosin
595 concentrations, indicative of a higher duty ratio, despite having a smaller working stroke. **A)**
596 shows the measured speed and **B)** shows normalized data. ~40 filaments were tracked
597 across four fields of view from two different experimental preparations. **C and D)** Regulated
598 i*n vitro* motility speed using thin filaments decorated with troponin and tropomyosin as a
599 function of calcium. The data were fitted with the Hill equation and the fitted values ±
600 standard error are: V_{max} values are 386 ± 8 vs. 135 ± 7 nm/s ($P < 0.001$), pCa50 values are
601 5.76 ± 0.02 vs. 6.1 ± 0.09 ($P = 0.01$), and the Hill coefficients are 3.4 ± 0.4 vs 3.1 ± 1.5 ($P =$
602 0.85) for the control vs. 10 μM danicamtiv, respectively **C)** Shows the measured speed and
603 **D)** shows the data normalized to the fitted V_{max} and V_{min}. Each point represents average
604 speed with error bars showing the standard deviation of ~40-60 filaments imaged from 4-6
605 fields of view from 2-3 experimental replicates. **E)** Simulated force-calcium relationship from
606 FiberSim. To simulate danicamtiv, we incorporated increased actin attachment, reduced
607 myosin working stroke, and an increase in the population of active myosin heads. The
608 simulations recapitulate the shift seen in the motility experiments. 5 replicates were
609 conducted, the shaded region shows the range of values, and the solid line shows the mean.
610 **F)** Simulated twitch in response to a calcium transient using the same simulation
611 parameters. Danicamtiv increases the maximal force, slows kinetics, and **G)** increases the
612 force-time integral.

613 **FIGURES**

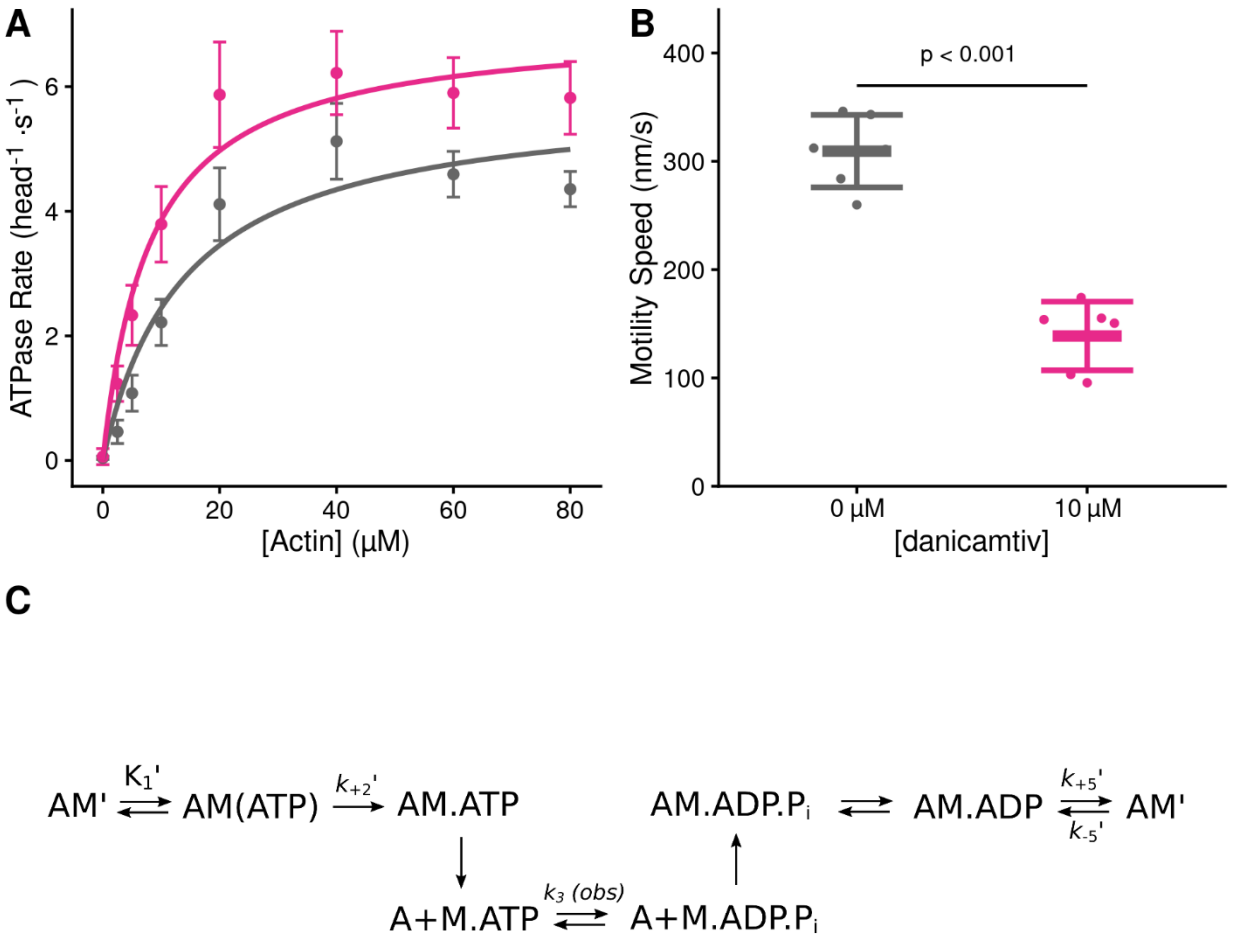

614

615 **Figure 1**

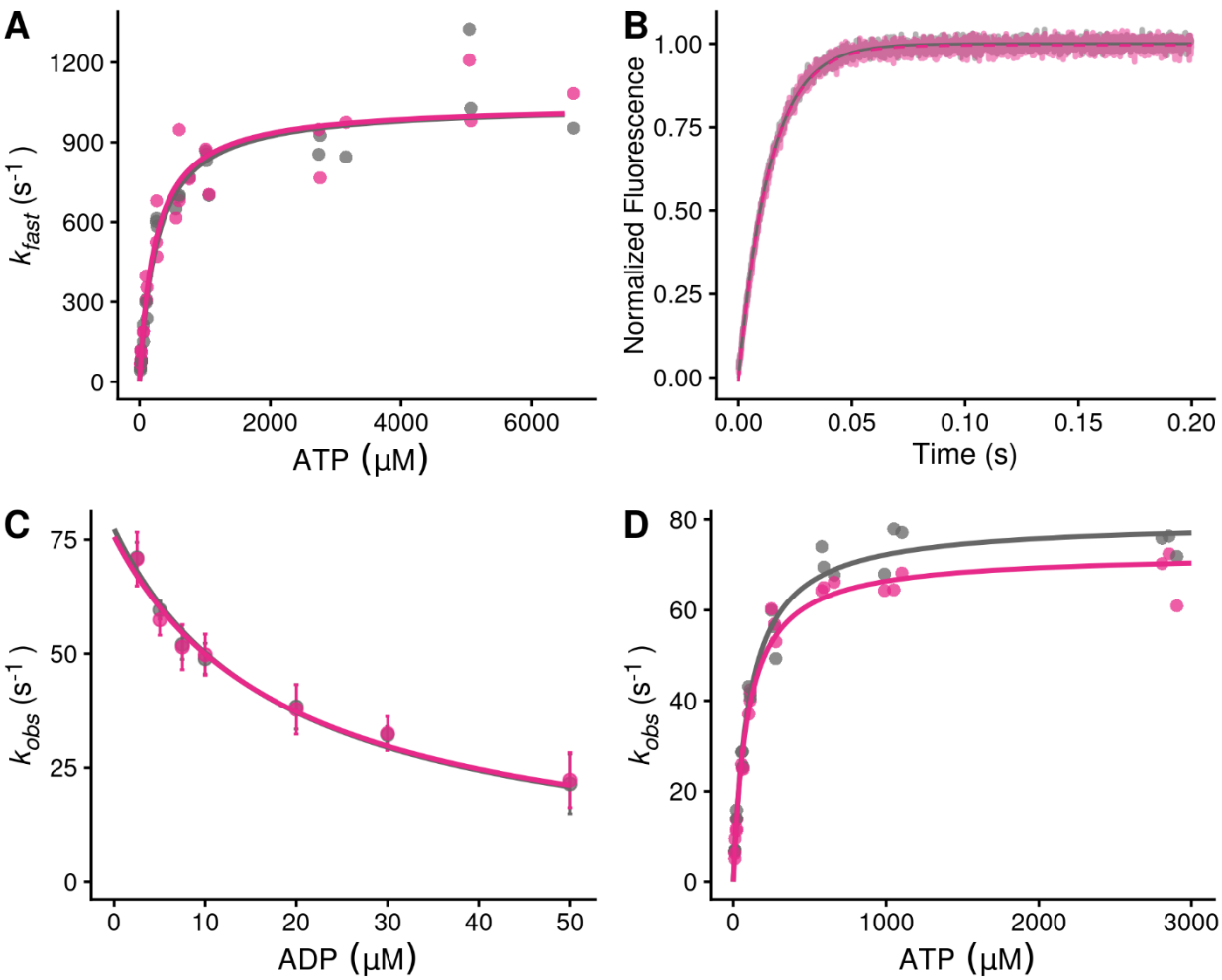

616

617 **Figure 2**

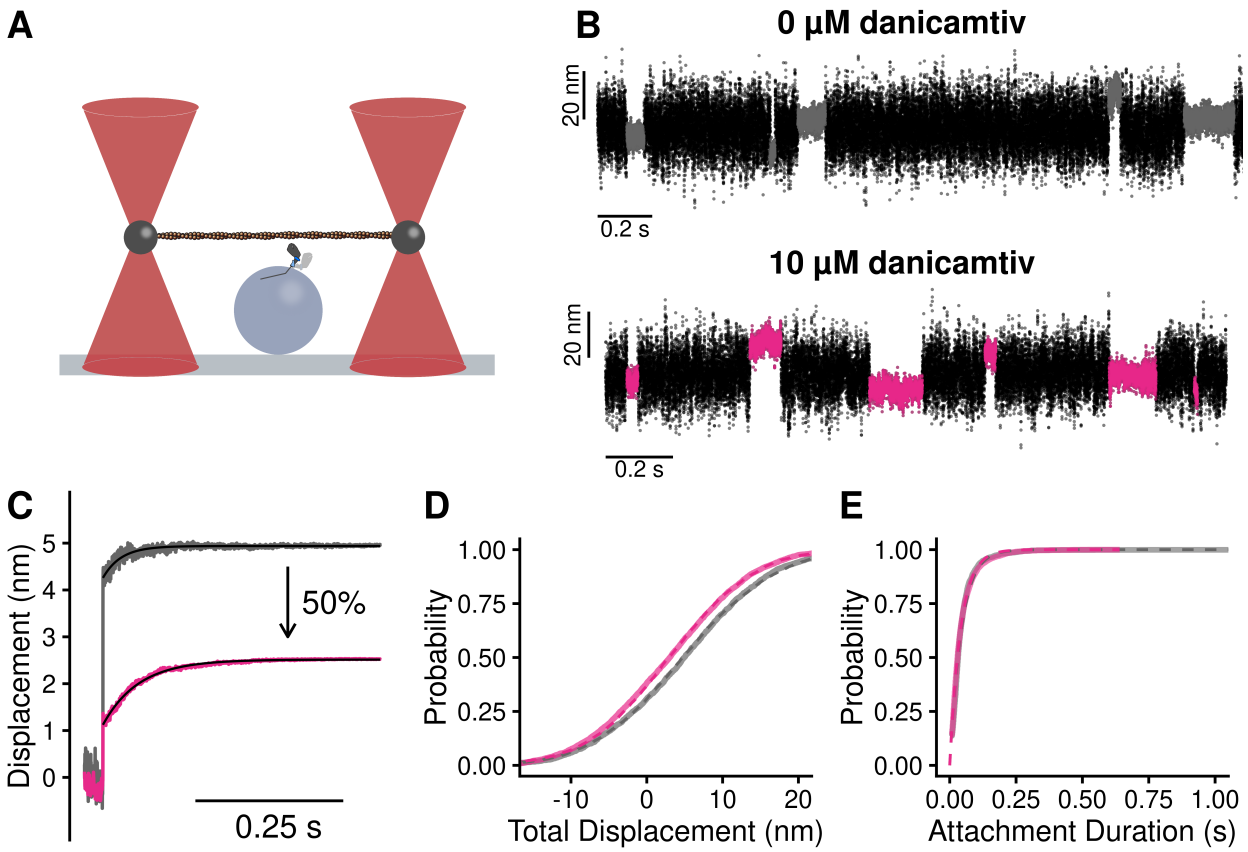

618

619 **Figure 3**

620

621

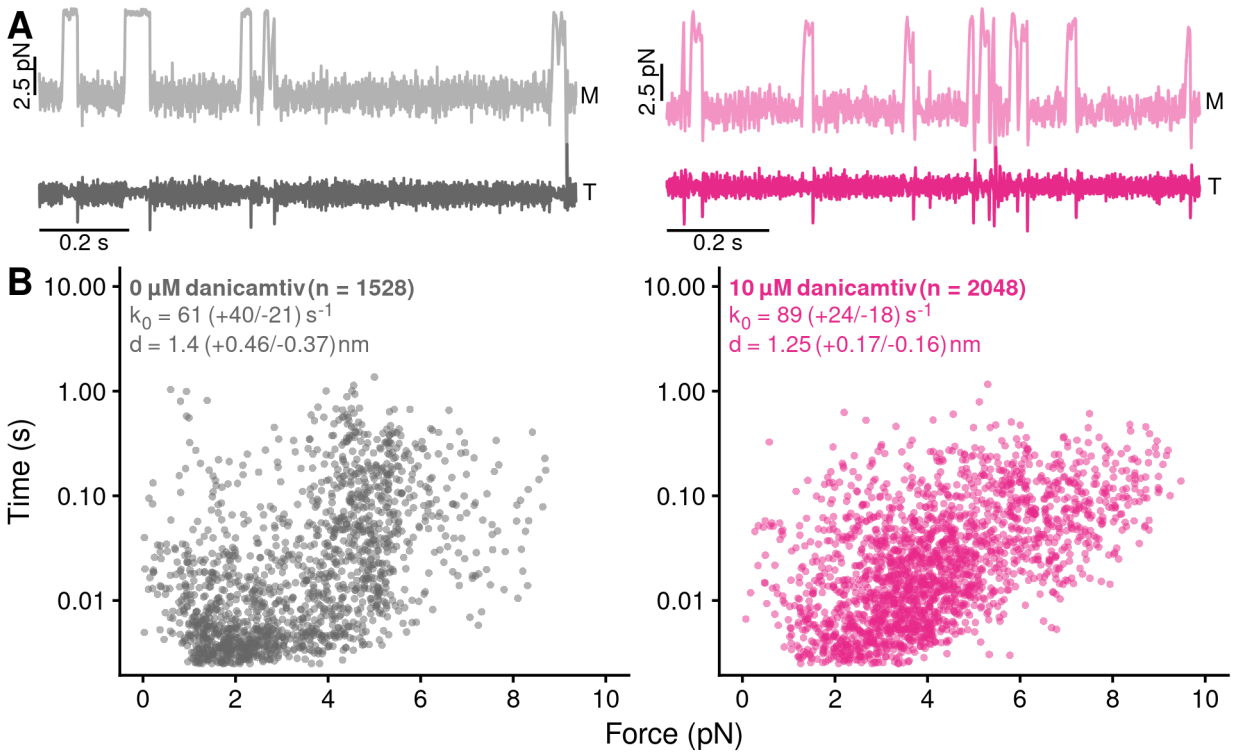
A
2.5 pN
M
T
0.2 s
2.5 pN
M
T
0.2 s
B
0 µM danicamtiv (n = 1528)
k0 = 61 (+40/-21) s-1
d = 1.4 (+0.46/-0.37) nm
10 µM danicamtiv (n = 2048)
k0 = 89 (+24/-18) s-1
d = 1.25 (+0.17/-0.16) nm
Time (s)
10.00
1.00
0.10
0.01
0
2
4
6
8
10
Force (pN)

Figure 4

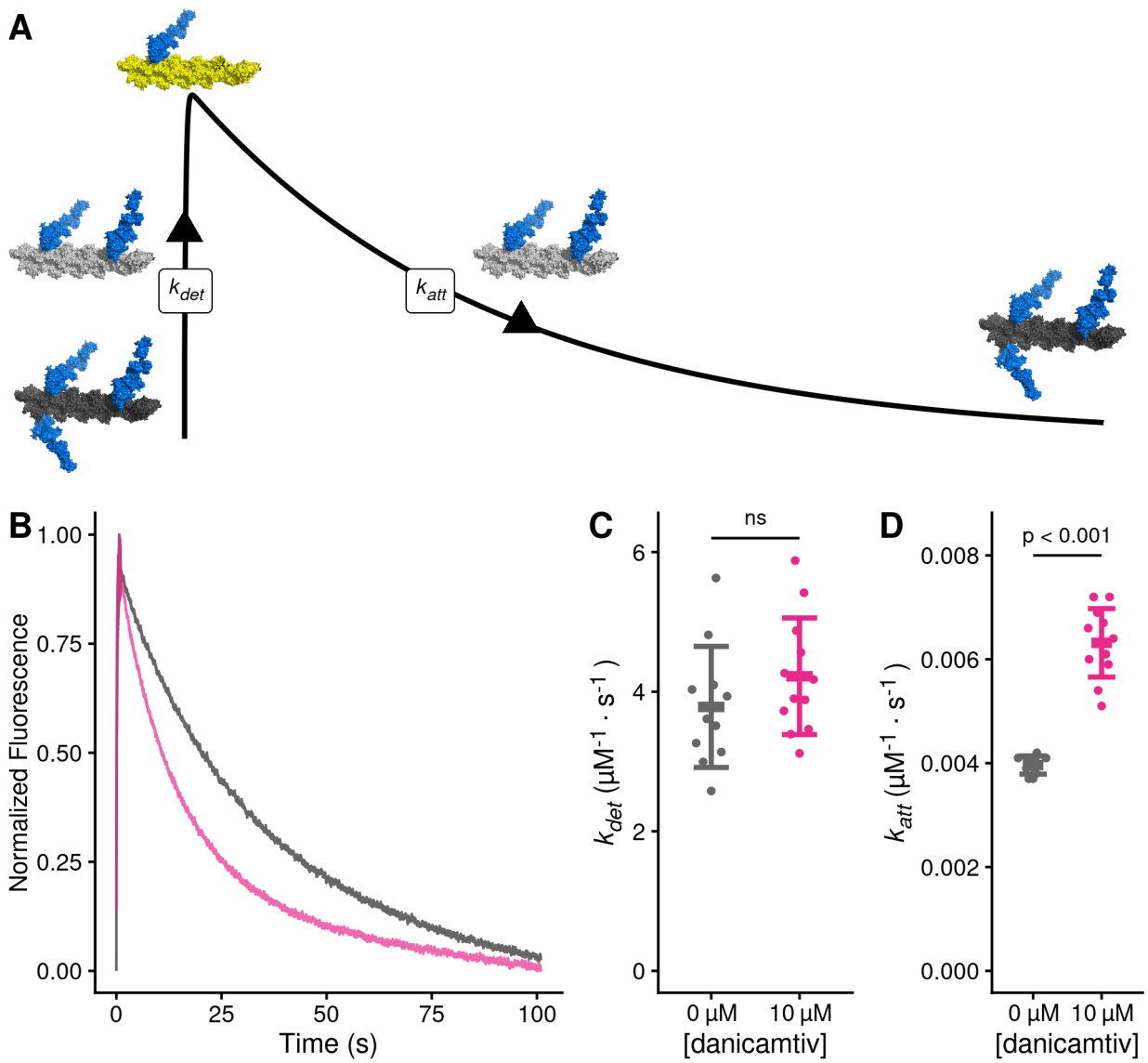
A
k_{det}
k_{att}
B
Normalized Fluorescence
1.00
0.75
0.50
0.25
0.00
0
25
50
75
100
Time (s)
C
ns
k_{det} (μM^{-1} · s^{-1})
6
4
2
0
0 μM
10 μM
[danicamtiv]
D
p < 0.001
k_{att} (μM^{-1} · s^{-1})
0.008
0.006
0.004
0.002
0.000
0 μM
10 μM
[danicamtiv]

Figure 5

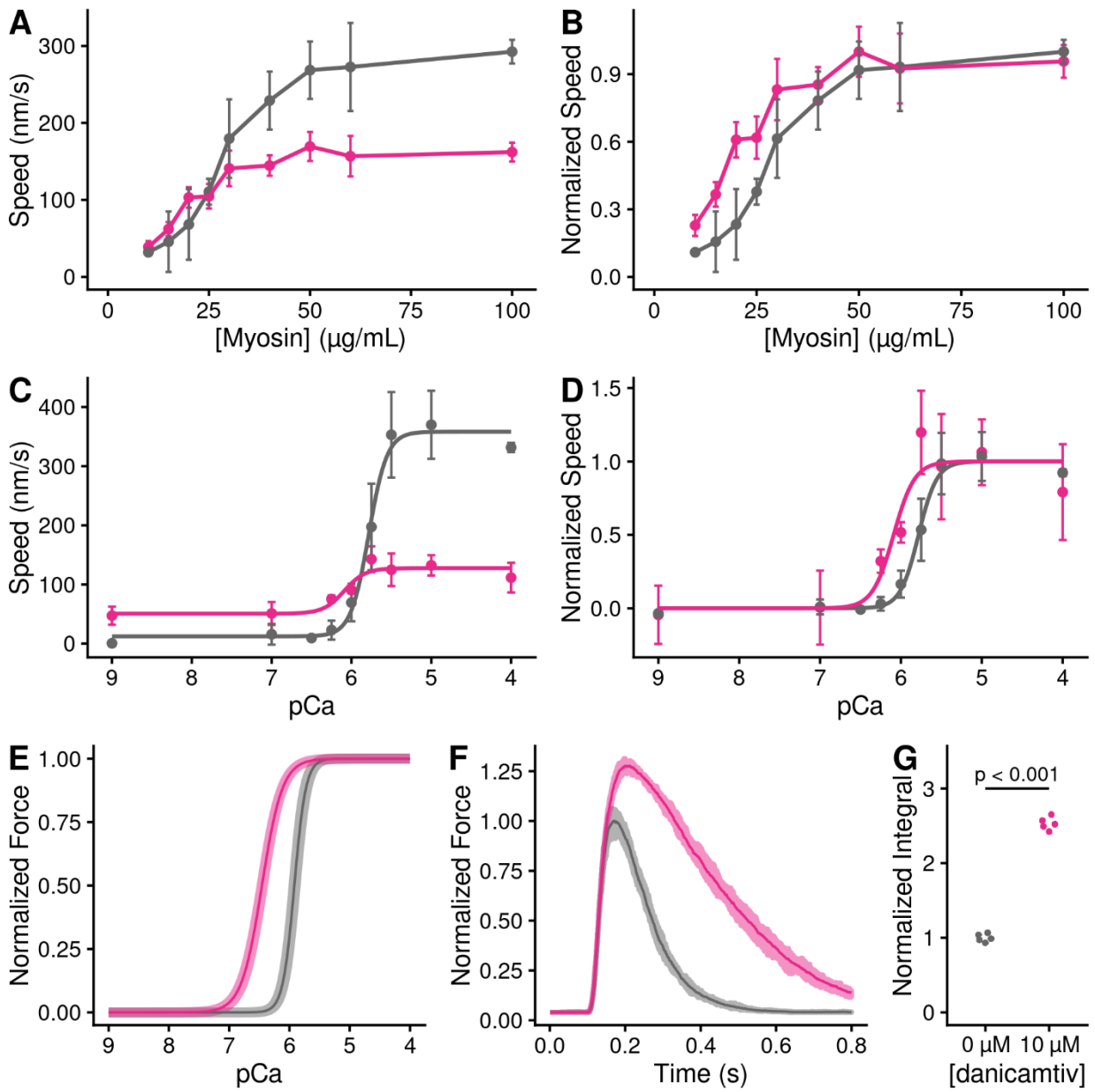

634

635 **Figure 6**

636

Table 1. Solution kinetics summary.

Parameter	0 μM danicamtiv	10 μM danicamtiv	P-value
Steady State ATPase			
V_{max} (head^{-1}·s^{-1})	5.9 ± 0.4	7.0 ± 0.6	0.028
K_m (μM)	14.0 ± 2.5	8.1 ± 1.6	0.01
Catalytic Efficiency [V_{max}/K_m] (μM^{-1}·s^{-1})*	0.42 ± 0.08	0.86 ± 0.19	0.013
ATP Induced Dissociation			
$1/K_1'$ (μM)	269 ± 71	245 ± 38	0.64
k_{+2}' (s^{-1})	1054 ± 123	1053 ± 86	0.99
$K_1'\cdot k_{+2}'$ (μM^{-1}·s^{-1})*	4.0 ± 0.7	4.4 ± 1.1	0.64
ADP Release			
k_{+5}' (s^{-1})	73.2 ± 3.3	73.1 ± 3.3	0.96
k_{-5}' (μM^{-1}·s^{-1})*	4.1 ± 0.3	3.9 ± 0.2	0.40
K_5' (μM)	18.0 ± 4.6	18.6 ± 4.1	0.87
ATP Hydrolysis			
k_3 *(obs)* (s^{-1})	79.8 ± 3.0	72.6 ± 2.5	0.03
Single turnover assay			
k_{det} (μM^{-1}·s^{-1})	3.8 ± 0.9	4.2 ± 0.8	0.23
k_{att} (μM^{-1}·s^{-1})	0.0040 ± 0.0002	0.0063 ± 0.0007	< 0.001

*calculated value

637

638

Table 2. Optical trap summary.

Parameter	0 μM danicamtiv	10 μM danicamtiv	P-value
10 uM ATP			
Total Step (nm)	4.9 ± 9.7	3.0 ± 9.0	< 0.001
Total Step (nm)*	5.0	2.5	
k_f (s^{-1})*	51	26	
Detachment Rate (s^{-1})	23 (-2.5/+2.5)	24 (-0.8/+0.9)	0.39
Number of Events	2076	4776	
1 mM ATP			
Displacement (nm)	5.1 ± 6.8	2.6 ± 7.2	< 0.001
Detachment Rate (s^{-1})	41.4 (-6.6/+6.8)	34.2 (-5.7/+7.1)	0.15
Number of Events	965	1695	
Isometric Force Clamp			
k_0 (s^{-1})	61 (-21/+40)	89 (-18/+24)	0.12
d (nm)	1.40 (-0.37/+0.46)	1.25 (-0.16/+0.17)	0.35
Number of Events	1755	2107	

*ensemble average fit parameter

639

References

1. P. A. Heidenreich *et al.*, 2022 AHA/ACC/HFSA Guideline for the Management of Heart Failure: Executive Summary: A Report of the American College of Cardiology/American Heart Association Joint Committee on Clinical Practice Guidelines. *J Am Coll Cardiol* **79**, 1757-1780 (2022).
2. E. M. Hsich *et al.*, Heart Transplantation: An In-Depth Survival Analysis. *JACC Heart Fail* **8**, 557-568 (2020).
3. J. G. Rogers *et al.*, Chronic mechanical circulatory support for inotrope-dependent heart failure patients who are not transplant candidates: results of the INTrEPID Trial. *J Am Coll Cardiol* **50**, 741-747 (2007).
4. E. M. Green *et al.*, A small-molecule inhibitor of sarcomere contractility suppresses hypertrophic cardiomyopathy in mice. *Science* **351**, 617-621 (2016).
5. F. I. Malik *et al.*, Cardiac myosin activation: a potential therapeutic approach for systolic heart failure. *Science* **331**, 1439-1443 (2011).
6. B. P. Morgan *et al.*, Discovery of omecamtiv mecarbil the first, selective, small molecule activator of cardiac Myosin. *ACS Med Chem Lett* **1**, 472-477 (2010).
7. H. He *et al.*, Novel Small-Molecule Troponin Activator Increases Cardiac Contractile Function Without Negative Impact on Energetics. *Circ Heart Fail* **15**, e009195 (2022).
8. S. J. Lehman, C. Crocini, L. A. Leinwand, Targeting the sarcomere in inherited cardiomyopathies. *Nat Rev Cardiol* **19**, 353-363 (2022).
9. S. Shen, L. R. Sewanan, D. L. Jacoby, S. G. Campbell, Danicamtiv Enhances Systolic Function and Frank-Starling Behavior at Minimal Diastolic Cost in Engineered Human Myocardium. *J Am Heart Assoc* **10**, e020860 (2021).
10. J. R. Teerlink *et al.*, Cardiac Myosin Activation with Omecamtiv Mecarbil in Systolic Heart Failure. *N Engl J Med* **384**, 105-116 (2021).
11. A. A. Voors *et al.*, Effects of danicamtiv, a novel cardiac myosin activator, in heart failure with reduced ejection fraction: experimental data and clinical results from a phase 2a trial. *Eur J Heart Fail* **22**, 1649-1658 (2020).
12. P. O. Awinda, B. J. Vander Top, K. L. Turner, B. C. W. Tanner, Danicamtiv affected isometric force and cross-bridge kinetics similarly in skinned myocardial strips from male and female rats. *J Muscle Res Cell Motil* **45**, 115-122 (2024).
13. J. Choi, J. B. Holmes, K. S. Campbell, J. E. Stelzer, Effect of the Novel Myotrope Danicamtiv on Cross-Bridge Behavior in Human Myocardium. *J Am Heart Assoc* **12**, e030682 (2023).
14. K. B. Kooiker *et al.*, Danicamtiv Increases Myosin Recruitment and Alters Cross-Bridge Cycling in Cardiac Muscle. *Circ Res* **133**, 430-443 (2023).
15. M. S. Woody *et al.*, Positive cardiac inotrope omecamtiv mecarbil activates muscle despite suppressing the myosin working stroke. *Nat Commun* **9**, 3838 (2018).
16. S. R. Clippinger Schulte *et al.*, Single-molecule mechanics and kinetics of cardiac myosin interacting with regulated thin filaments. *Biophys J* **122**, 2544-2555 (2023).
17. C. Liu, M. Kawana, D. Song, K. M. Ruppel, J. A. Spudich, Controlling load-dependent kinetics of beta-cardiac myosin at the single-molecule level. *Nat Struct Mol Biol* **25**, 505-514 (2018).
18. S. J. Kron, J. A. Spudich, Fluorescent actin filaments move on myosin fixed to a glass surface. *Proc Natl Acad Sci U S A* **83**, 6272-6276 (1986).
19. J. A. Spudich, Hypertrophic and dilated cardiomyopathy: four decades of basic research on muscle lead to potential therapeutic approaches to these devastating genetic diseases. *Biophys J* **106**, 1236-1249 (2014).
20. S. K. Barrick, M. J. Greenberg, Cardiac myosin contraction and mechanotransduction in health and disease. *J Biol Chem* **297**, 101297 (2021).

21. E. M. De La Cruz, E. M. Ostap, Kinetic and equilibrium analysis of the myosin ATPase. *Methods Enzymol* **455**, 157-192 (2009).
22. S. R. Clippinger *et al.*, Disrupted mechanobiology links the molecular and cellular phenotypes in familial dilated cardiomyopathy. *Proc Natl Acad Sci U S A* **116**, 17831-17840 (2019).
23. J. C. Deacon, M. J. Bloemink, H. Rezavandi, M. A. Geeves, L. A. Leinwand, Identification of functional differences between recombinant human alpha and beta cardiac myosin motors. *Cell Mol Life Sci* **69**, 2261-2277 (2012).
24. T. Blackwell, W. T. Stump, S. R. Clippinger, M. J. Greenberg, Computational Tool for Ensemble Averaging of Single-Molecule Data. *Biophys J* **120**, 10-20 (2021).
25. J. T. Finer, R. M. Simmons, J. A. Spudich, Single myosin molecule mechanics: piconewton forces and nanometre steps. *Nature* **368**, 113-119 (1994).
26. M. J. Greenberg, H. Shuman, E. M. Ostap, Inherent force-dependent properties of beta-cardiac myosin contribute to the force-velocity relationship of cardiac muscle. *Biophys J* **107**, L41-L44 (2014).
27. M. J. Greenberg, H. Shuman, E. M. Ostap, Measuring the Kinetic and Mechanical Properties of Non-processive Myosins Using Optical Tweezers. *Methods Mol Biol* **1486**, 483-509 (2017).
28. T. Lin, M. J. Greenberg, J. R. Moore, E. M. Ostap, A hearing loss-associated myo1c mutation (R156W) decreases the myosin duty ratio and force sensitivity. *Biochemistry* **50**, 1831-1838 (2011).
29. T. Q. Uyeda, S. J. Kron, J. A. Spudich, Myosin step size. Estimation from slow sliding movement of actin over low densities of heavy meromyosin. *J Mol Biol* **214**, 699-710 (1990).
30. D. E. Harris, D. M. Warshaw, Smooth and skeletal muscle myosin both exhibit low duty cycles at zero load in vitro. *J Biol Chem* **268**, 14764-14768 (1993).
31. D. F. McKillop, M. A. Geeves, Regulation of the interaction between actin and myosin subfragment 1: evidence for three states of the thin filament. *Biophys J* **65**, 693-701 (1993).
32. D. M. Bers, Cardiac excitation-contraction coupling. *Nature* **415**, 198-205 (2002).
33. S. Kosta, D. Colli, Q. Ye, K. S. Campbell, FiberSim: A flexible open-source model of myofilament-level contraction. *Biophys J* **121**, 175-182 (2022).
34. S. Weiss, R. Rossi, M. A. Pellegrino, R. Bottinelli, M. A. Geeves, Differing ADP release rates from myosin heavy chain isoforms define the shortening velocity of skeletal muscle fibers. *J Biol Chem* **276**, 45902-45908 (2001).
35. A. P. Raduly *et al.*, The Novel Cardiac Myosin Activator Danicamtiv Improves Cardiac Systolic Function at the Expense of Diastolic Dysfunction In Vitro and In Vivo: Implications for Clinical Applications. *Int J Mol Sci* **24** (2022).
36. M. J. Greenberg, J. C. Tardiff, Complexity in genetic cardiomyopathies and new approaches for mechanism-based precision medicine. *J Gen Physiol* **153** (2021).
37. Y. Liu, H. D. White, B. Belknap, D. A. Winkelmann, E. Forgacs, Omecamtiv Mecarbil modulates the kinetic and motile properties of porcine beta-cardiac myosin. *Biochemistry* **54**, 1963-1975 (2015).
38. L. Greenberg *et al.*, Harnessing molecular mechanism for precision medicine in dilated cardiomyopathy caused by a mutation in troponin T. *bioRxiv* 10.1101/2024.04.05.588306 (2024).
39. S. R. Clippinger *et al.*, Mechanical dysfunction of the sarcomere induced by a pathogenic mutation in troponin T drives cellular adaptation. *J Gen Physiol* **153** (2021).
40. S. K. Barrick, L. Greenberg, M. J. Greenberg, A troponin T variant linked with pediatric dilated cardiomyopathy reduces the coupling of thin filament activation to myosin and calcium binding. *Mol Biol Cell* **32**, 1677-1689 (2021).